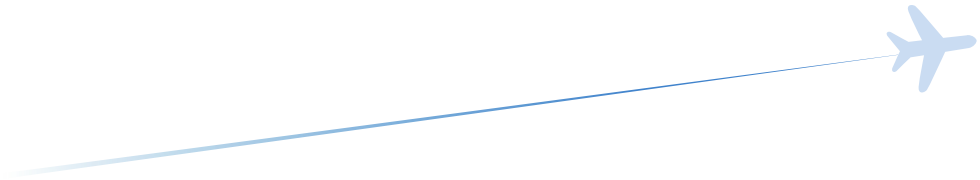

Methodology to assess the uncertainty of sector demand

Deliverable 5.1

TBO-Met

Grant:	**699294**
Call:	**H2020-SESAR-2015-1**
Topic:	**Sesar-04-2015 - Environment and Meteorology in ATM**
Consortium coordinator:	**University of Seville**
Edition date:	**23 March 2017**
Edition:	**00.01.01**

Founding Members

EUROPEAN UNION EUROCONTROL

SESAR JOINT UNDERTAKING

Authoring & Approval

Authors of the document

Name/Beneficiary	Position/Title	Date
Alfonso Valenzuela / USE	USE contributor	21/02/2017
Antonio Franco / USE	USE contributor	21/02/2017
Damian Rivas / USE	USE contribution leader	21/02/2017

Reviewers internal to the project

Name/Beneficiary	Position/Title	Date
Damian Rivas / USE	USE contribution leader	27/02/2017
Manuel Soler / UC3M	UC3M contribution leader	27/02/2017
Jürgen Lang / MetSol	MetSol contribution leader	27/02/2017
Carl-Herbert Rokitansky / PLUS	PLUS contribution leader	27/02/2017
Juan Simarro / AEMET	AEMET contribution leader	27/02/2017

Approved for submission to the SJU By — Representatives of beneficiaries involved in the project

Name/Beneficiary	Position/Title	Date
Alfonso Valenzuela / USE	USE contributor	23/03/2017
Antonio Franco / USE	USE contributor	23/03/2017
Damian Rivas / USE	Project Coordinator	23/03/2017

Rejected By - Representatives of beneficiaries involved in the project

Name/Beneficiary	Position/Title	Date

Document History

Edition	Date	Status	Author	Justification
00.00.01	21/02/2017	Initial Draft	A. Valenzuela	New document
00.01.00	27/02/2017	First Issue	A. Valenzuela	Updated document
00.01.01	23/03/2017	Revised Issue	A. Valenzuela	Reviewed following SJU assessment report

TBO-Met

METEOROLOGICAL UNCERTAINTY MANAGEMENT FOR TRAJECTORY BASED OPERATIONS

This deliverable is part of a project that has received funding from the SESAR Joint Undertaking under grant agreement No 699294 under European Union's Horizon 2020 research and innovation programme.

Abstract

In this deliverable, the methodology to assess the uncertainty of sector demand is presented. The methodology requires the definition of a scenario (in terms of Air Traffic Control sector, flights, and weather forecasts to be considered), the processing of meteorological data (provided by Ensemble Prediction Systems and Nowcasts, which are composed of different possible atmosphere realizations), and a trajectory predictor (which, for each flight and for each atmosphere realization, computes a different aircraft trajectory). The computed trajectories, along with the information of the sector, are then used to analyse the sector demand, which is described in terms of entry count (number of flights entering the sector during a selected time period) and of occupancy count (number of flights inside the sector during a selected time period). The analysis is based on the statistical characterization of the entry and exit times of the flights to/from the sector, and of the entry and occupancy counts. The probability of the counts exceeding the declared capacity of the sector is obtained. A realistic application example is included in this deliverable to show the potentiality of the methodology, using a trajectory predictor that has been specifically developed for this example. This application clearly shows the suitability of the methodology for the purpose of TBO-Met.

Table of Contents

1 Executive Summary 5
2 Introduction 6
3 Methodology 9
4 Application Example 16
5 Conclusions 39
6 References 41

1 Executive Summary

In this deliverable, the methodology to assess the uncertainty of sector demand when meteorological uncertainty is taken into account is presented. This methodology will be applied in later stages of the project to quantify the effects of weather uncertainty on the sector demand at the pre-tactical and tactical levels (that is, mid- and short-term planning and execution), and to quantify the benefits of improving the predictability of individual trajectories on the predictability of sector demand, which are the main objectives of Work Package (WP) 5.

The developed methodology is presented in Section 3. It starts from the definition of the scenario in terms of Air Traffic Control (ATC) sector, flights, and weather forecasts to be considered. In TBO-Met, the meteorological uncertainty is provided by Ensemble Prediction Systems (EPS) and Nowcasts, which consider different possible atmosphere realizations. A trajectory predictor computes, for each flight and for each atmosphere realization, a different aircraft trajectory. The computed trajectories, along with the information of the ATC sector, are then used to analyse the sector demand. The methodology is general, in the sense that it is applicable regardless the source of weather uncertainty (EPS or Nowcasts) and the forecast horizon (pre-tactical or tactical level). In TBO-Met, the processing of the meteorological data is addressed in WP 2, and the development of trajectory predictors for the pre-tactical and tactical phases is done in WP 4.

The sector demand is described in terms of entry count (number of flights entering the sector during a selected time period) and of occupancy count (number of flights inside the sector during a selected time period). The analysis is based on the statistical characterization of the entry and exit times of the flights to/from the sector, and of the entry and occupancy counts. The probability of the counts exceeding given thresholds is obtained.

In Section 4, a realistic application example to show the potentiality of the methodology is provided. The demand of the ATC sector LECMSAU is analysed for a whole day when predicted the day before. The meteorological uncertainty is retrieved from the European Centre for Medium-Range Weather Forecasts (ECMWF) and provided by the ensemble forecast ECMWF-EPS. A trajectory predictor which takes into account the uncertainty in wind and air temperature has been specifically developed for this application. In this particular example, it has been found that those flights that travel a larger distance to the entry point, to the exit point, and inside the sector, have a higher uncertainty in the entry, exit, and occupancy times, respectively. It is also found that the uncertainty in the entry count is rather large when compared with the declared capacity of the sector.

2 Introduction[1]

As described in the Grant Agreement [1], the general objective of WP 5 is to increase the accuracy of the prediction of sector demand when meteorological uncertainty is taken into account. In particular, the following sub-objectives are considered:

1. To understand how weather uncertainty is propagated from the trajectory scale to the traffic scale.
2. To quantify the effects of weather uncertainty on the sector demand at the pre-tactical and tactical phases.
3. To quantify the benefits of improving the predictability of individual trajectories on the predictability of sector demand.

In TBO-Met, the meteorological uncertainty is provided by Ensemble Prediction Systems (EPS) at the pre-tactical level (mid-term planning) [2] and by EPS and Nowcasts at the tactical level (short-term planning and execution) [3].

Typically, an EPS is a collection of 10 to 50 forecasts, referred to as members, with forecasting horizons of up to 2-5 days. They consist on running many times a deterministic model from very slightly different initial conditions [4]. Often, the model physics is also slightly perturbed, and some ensembles use more than one model within the ensemble or the same model but with different combinations of physical parameterization schemes. This technique generates a representative sample of the possible realizations of the potential weather outcome. The uncertainty information is on the spread of the solutions in the ensemble, and the hope is that the spread of the predictions in the ensemble brackets the true weather outcome [5].

Nowcasts are short-term forecasts, up to 1-3 hours, based on the actually observed situation. They usually use radar or satellite data, some in combination with wind data, and extrapolate the movement and the temporal development of small scale weather phenomena like thunderstorms [6, 7], which are not precisely forecasted by numerical weather prediction models and EPS. Nowcast systems work on the regional scale and are quite reliable for one hour lead time with decreasing accuracy for longer times. However, since Nowcasts rely on already existing weather phenomena, they do not forecast emerging weather features.

Uncertain trajectories are expected to be obtained during the process of trajectory planning when meteorological uncertainty is taken into account. One of the objectives of WP 4 is to develop

[1] The opinions expressed herein reflect the author's view only. Under no circumstances shall the SESAR Joint Undertaking be responsible for any use that may be made of the information contained herein.

algorithms capable of providing more predictable trajectories at the cost of losing efficiency, e.g. increasing the fuel consumption.

In TBO-Met, the sector demand is described in terms of entry count and of occupancy count. The entry count is defined as the number of flights entering the sector during a selected time period, whereas the occupancy count is defined as the number of flights inside the sector during a selected time period [8]. Both counts, entry and occupancy counts, are obtained from the intersections of the individual aircraft trajectories with the geometry of the sector. Since the aircraft trajectories are expected to be uncertain, then the associated entry and exit times are also uncertain and, thus, the entry and occupancy counts are also expected to be uncertain.

In this deliverable, the methodology to assess the uncertainty of sector demand is presented, see Section 3. This methodology allows to obtain the entry and occupancy counts, and statistical properties related to them, from uncertain trajectories. The methodology is general, in the sense that it is suitable to all the applications considered in TBO-Met, regardless the source of weather uncertainty (EPS or Nowcasts) and the forecast horizon (pre-tactical or tactical level, that is, mid- and short-term planning and execution). The only requisite is to have a finite number of possible trajectories for each aircraft, each trajectory corresponding to a different weather prediction. An example of the application of this methodology is given in Section 4.

In deliverable D5.2 (“Effects of weather uncertainty in sector demand”), the developed methodology will be applied to quantify the effects of weather uncertainty on the sector demand at the pre-tactical and tactical phases taking the input provided by WP 4. The benefits of improving the predictability of individual trajectories on the predictability of sector demand when the trajectories are improved according to the algorithms developed in WP 4 will be also quantified. According to the Project Management Plan [9], the due date of this deliverable is T0+18 (30/11/2017).

2.1 Acronyms and Terminology

Term	Definition
AIRAC	Aeronautical Information Regulation and Control
ATC	Air Traffic Control
ATFCM	Air Traffic Flow and Capacity Management
BADA	Base of Aircraft Data
ECMWF	European Centre for Medium-Range Weather Forecasts
EPS	Ensemble Prediction System
Met	Meteorology
NEST	Network Strategic Tool
TBO	Trajectory Based Operations

WP	Work Package

TBO-Met Consortium

AEMET	Agencia Estatal de Meteorología
MetSol	MeteoSolutions GmbH
PLUS	University of Salzburg
UC3M	University Carlos III of Madrid
USE	University of Seville

3 Methodology

The general scheme to be followed in TBO-Met for the analysis of sector demand is shown in Figure 1. Initially, the scenarios have to be defined, in terms of: 1) ATC sector (e.g., geometry and capacity), 2) flights that cross the sector (e.g., origin and destination, route, departure time, flight levels, and cruise speeds), and 3) weather forecast (e.g., EPSs or Nowcasts to be considered, release time, and forecast times).

The meteorological data provided by the weather forecasts are then processed for its use by the trajectory predictor. For example, the necessary values of wind and air temperature are extracted, and information about convection is derived from numerous parameters. The data processing developed in TBO-Met in WP 2 is described in deliverables D2.1 [2] and D2.3 [3].

The trajectory predictor computes, for each flight and for each weather prediction, a different aircraft trajectory. The trajectory predictor developed in WP 4 for the pre-tactical level (mid- term planning) is described in deliverable D4.1 [10], whereas the trajectory predictor developed for the tactical level (short-term planning and execution) will be presented in deliverable D4.2. The trajectory predictor specifically developed for the example of this deliverable is described in Section 4.2.

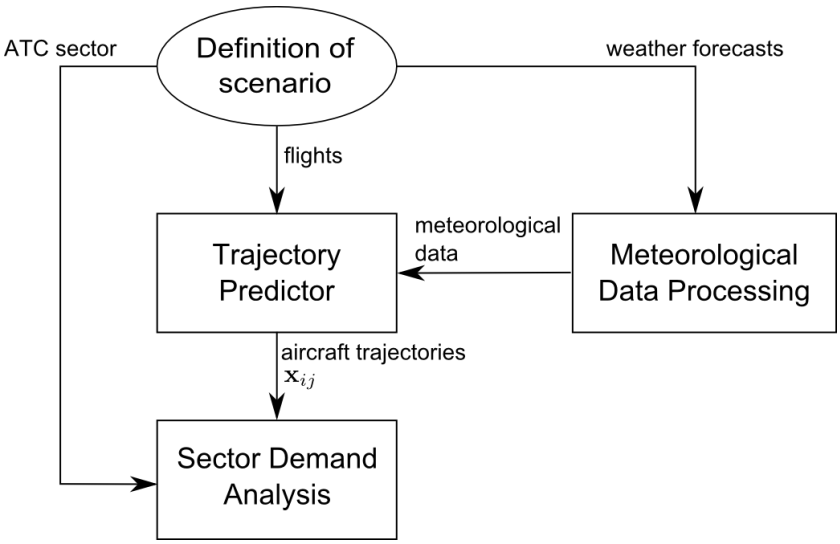

Figure 1. General scheme for the analysis of sector demand.

The computed trajectories, along with the information of the ATC sector, are then used to perform the analysis of the sector demand. The different atmospheric realizations, in terms of wind and air temperature, lead to different predicted entry and exit times, and, therefore, to different occupancy and entry counts.

The analysis is based on the statistical characterization of the entry and exit times of the flights to/from the sector, and of the entry and occupancy counts. For example, mean, maximum, or minimum values, or the spread of these time and counts, measured as the difference between the maximum and minimum values, are examined. The analysis also allows to determine which flights contribute the most to the demand uncertainty. Finally, the probability of the counts exceeding given thresholds is also obtained, which can be used to represent the probability that the demand exceeds the capacity of the ATC sector. This probability can be useful in the Demand-Capacity Balancing process. The higher the value of the probability and the capacity deficit, the more severe the Air Traffic Flow and Capacity Management (ATFCM) measure to be considered.

Next, some definitions are provided and the general hypotheses are established. Following, the entry, exit, and occupancy times and distances are described, obtained from the individual aircraft trajectories. Finally, the entry and the occupancy counts are also described, obtained from the previous times.

3.1 Definitions and General Hypotheses

The position of any point in the space is given by its coordinates: λ (longitude), ϕ (latitude), and h (pressure altitude). The methodology is independent of the geodetic system the longitude and latitude are referred to, e.g. spherical or ellipsoidal Earth.

R is the airspace of the ATC sector, a volume in the λ, ϕ, h-space, and ∂R is the contour of the ATC sector (i.e. the contour of R), a surface in the λ, ϕ, h-space. In TBO-Met, it is considered that this geometry is fixed and does not change with time; therefore, the effects of opening/closing sectors are not analysed.

It is considered that there exist m different flights and that the EPS or Nowcast is formed by n different members or atmospheric realizations. The position of flight i ($i = 1, \dots, m$) for member j ($j = 1, \dots, n$) at time t, is denoted as $\mathbf{x}_{ij}(t)$. It is given by the longitude, the latitude, and the pressure altitude:

$$\mathbf{x}_{ij}(t) = \left[\lambda_{ij}(t), \phi_{ij}(t), h_{ij}(t)\right]. \tag{1}$$

The trajectories $\mathbf{x}_{ij}$ generated by WP 4 will be provided as a list of discrete points and times. A linear interpolation will be used to obtain the position of the flight at any time.

In TBO-Met, it is considered that the trajectory crosses the ATC sector only once; trajectories crossing the same sector multiple times are not considered (for example, flights that return to the departure airport) since this is an uncommon practice in commercial aviation.

It is worth noting that, for a given flight i, in the pre-tactical analysis the same route is expected for all members, whereas in the case of short-term planning and execution different routes may be obtained.

In this latter case, it may happen that for a given member j the trajectory $\mathbf{x}_{ij}$ does not cross the sector, and therefore it must be discarded for the analysis.

3.2 Entry, exit and occupancy times and distances

If trajectory $\mathbf{x}_{ij}$ crosses the ATC sector, then there exist an entry time to the sector $t_{ij,E}$ and an exit time from the sector $t_{ij,X}$ ($t_{ij,E} \leq t_{ij,X}$), and the associated entry and exit points, $\mathbf{x}_{ij}(t_{ij,E})$ and $\mathbf{x}_{ij}(t_{ij,X})$. The occupancy time for the flight i and for the ensemble member j, $t_{ij,O}$, is defined as the difference between the exit and the entry times

$$t_{ij,O} = t_{ij,X} - t_{ij,E}. \tag{2}$$

The entry, exit, and occupancy times can be statistically characterized. For flight i, we define the average entry, exit, and occupancy times ($t_{i,E}$, $t_{i,X}$ and $t_{i,O}$, respectively) as

$$t_{i,E} = \frac{1}{n}\sum_{j=1}^{n} t_{ij,E}, \tag{3}$$

$$t_{i,X} = \frac{1}{n}\sum_{j=1}^{n} t_{ij,X}, \tag{4}$$

$$t_{i,O} = \frac{1}{n}\sum_{j=1}^{n} t_{ij,O}. \tag{5}$$

The uncertainty information is on the spread of these times. The dispersion of the entry, exit, and occupancy times for flight i, ($\Delta t_{i,E}$, $\Delta t_{i,X}$, and $\Delta t_{i,O}$, respectively) are defined as the differences between the maximum and the minimum values for the different atmospheric realizations

$$\Delta t_{i,E} = \max_j t_{ij,E} - \min_j t_{ij,E}, \tag{6}$$

$$\Delta t_{i,X} = \max_j t_{ij,X} - \min_j t_{ij,X}, \tag{7}$$

$$\Delta t_{i,O} = \max_j t_{ij,O} - \min_j t_{ij,O}. \tag{8}$$

For flight i and for ensemble member j, the distance travelled by the aircraft from its origin to the entry point is denoted as $d_{ij,E}$, and the distance to the exit point as $d_{ij,X}$. Since the trajectories will be provided as a list of discrete points, the distance between two consecutive points is calculated considering a rhumb line (see, for example, Section 4.2). The distance flown inside the sector, $d_{ij,O}$, is the difference between these two distances

$$d_{ij,O} = d_{ij,X} - d_{ij,E}. \tag{9}$$

These distances can be also statistically characterized. The average values and the dispersions are defined as follows

$$d_{i,E} = \frac{1}{n}\sum_{j=1}^{n} d_{ij,E}, \tag{10}$$

$$d_{i,X} = \frac{1}{n}\sum_{j=1}^{n} d_{ij,X}, \tag{11}$$

$$d_{i,O} = \frac{1}{n}\sum_{j=1}^{n} d_{ij,O}, \tag{12}$$

$$\Delta d_{i,E} = \max_j d_{ij,E} - \min_j d_{ij,E}, \tag{13}$$

$$\Delta d_{i,X} = \max_j d_{ij,X} - \min_j d_{ij,X}, \tag{14}$$

$$\Delta d_{i,O} = \max_j d_{ij,O} - \min_j d_{ij,O}. \tag{15}$$

If it happens that for a particular member the trajectory does not cross the sector, then the entry and exit times and distances are not defined, and as consequence, this member is not considered for the computation of mean and dispersion values.

3.3 Entry count

The entry count for a given sector is defined as the number of flights entering the sector during a selected time period P_k,

$$P_k = [kt_s, kt_s + \delta t), \qquad k = 0,1,2,\ldots \tag{16}$$

where t_s is a step value that defines the time difference between the start times of two consecutive time periods, and δt is the duration of each time period. To clarify this definition, in Figure 2 a deterministic example of the entry and exit times of eight flights, and four time periods, with $\delta t = 2t_s$, is given. In this example, it is obtained that the entry count is 3 flights for period P_0 (flights 3, 4, and 5), 3 flights for period P_1 (flights 4, 5, and 6), 3 flights for period P_2 (flights 6, 7, and 8), and 2 flights for period P_3 (flights 7 and 8).

When the entry time is uncertain, then the entry count is also uncertain because the aircraft can enter the sector in different time periods. It is worth noting that the values of t_s and δt play a key role in the uncertainty of the entry count. If they are very small, then the aircraft can enter the sector in different time periods for different forecast members. As it will be seen in the example application (Section 4), the smaller the value of δt the higher the uncertainty in the entry count.

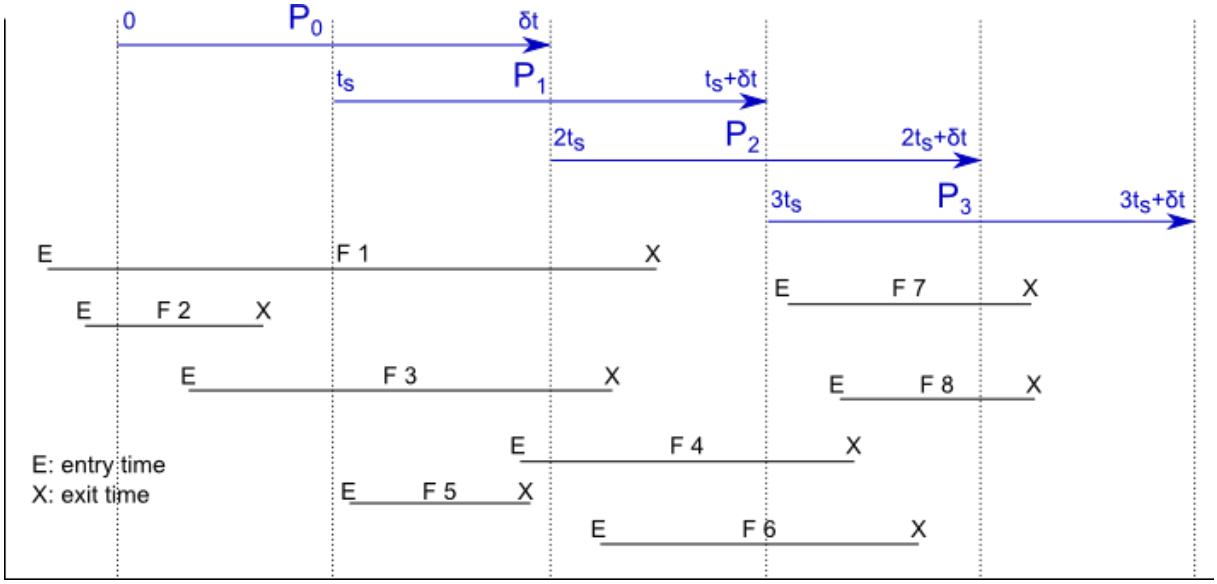

Figure 2. Example of entry and exit times for eight flights, and four time periods with $\delta t = 2t_s$. Adapted from Ref. [8].

We define an entry function for flight i, for ensemble member j, and for time period P_k, denoted as $E_{ij}(P_k)$. It takes the value 1 when the aircraft enters the ATC sector during this time period and the value 0 otherwise

$$E_{ij}(P_k) = \begin{cases} 1, & \text{if } t_{ij,E} \in P_k, \\ 0, & \text{otherwise.} \end{cases} \tag{17}$$

The entry count for ensemble member j and for time period P_k, denoted as $E_j(P_k)$, is obtained as the sum of the entries of the different flights

$$E_j(P_k) = \sum_{i=1}^{m} E_{ij}(P_k). \tag{18}$$

From these n values of the entry count, mean, maximum, and minimum values ($\bar{E}$, E_{max}, and E_{min}, respectively) for time period P_k can be determined

$$\bar{E}(P_k) = \frac{1}{n}\sum_{j=1}^{n} E_j(P_k), \tag{19}$$

$$E_{max}(P_k) = \max_j E_j(P_k), \tag{20}$$

$$E_{min}(P_k) = \min_j E_j(P_k). \tag{21}$$

The uncertainty information is on the spread of the entry count. The dispersion of the entry count, $\Delta E(P_k)$, is defined as follows

$$\Delta E(P_k) = E_{max}(P_k) - E_{min}(P_k). \tag{22}$$

The probability of the entry count E being greater than a given value a for time period P_k , e.g. the declared capacity, is obtained from the number of entry counts $E_j(P_k)$ that are greater than this value, as follows

$$P[E(P_k) > a] = \frac{\text{number of } E_j(P_k) > a}{n}. \tag{23}$$

Notice that, since the entry of each flight to the ATC sector for time period P_k only depends on the entry time $t_{ij,E}$, see Eq. (17), then the entry count and its statistical characterization are only affected by the uncertainty in this time. For one particular flight, the uncertainty in the entry time is expected to increase due to meteorological reasons when:

- the forecasting horizon increases,
- the aircraft flies over regions with high uncertainty before entering the sector, and
- the aircraft travels a large distance before entering the sector, thus accumulating uncertainty along the flight.

Correspondingly, the uncertainty in the entry count is expected to increase when:

- the entry count is computed far in advance,
- the aircraft are affected by meteorological phenomena with large uncertainty before entering the sector, and
- the traffic is composed of many flights arriving from distant locations.

3.4 Occupancy count

The occupancy count for a given sector is defined as the number of flights inside the sector during a selected time period P_k, defined as before, see Eq. (16). In the deterministic example given in Figure 2, the occupancy count is 5 flights for period P_0 (flights 1, 2, 3, 4, and 5), 5 flights for period P_1 (flights 1, 3, 4, 5, and 6), 6 flights for period P_2 (flights 1, 3, 4, 6, 7, and 8), and 4 flights for period P_3 (flights 4, 6, 7, and 8). As in the case of the entry count, when the entry and exit times are uncertain then the occupancy count is also uncertain because the aircraft can enter or exit the sector in different time periods for different forecast members.

We define an occupancy function for flight i, for ensemble member j, and for time period P_k, denoted as $O_{ij}(P_k)$. It takes the value 1 when the aircraft is inside the sector during this time period (it enters, exits, or stays in the sector in this period) and the value 0 if the aircraft is outside

$$O_{ij}(P_k) = \begin{cases} 1, & \text{if } \left(t_{ij,E} \in P_k\right) \text{ or } \left(t_{ij,X} \in P_k\right) \text{ or } \left(t_{ij,E} < kt_s \text{ and } t_{ij,X} \geq kt_s + \delta t\right), \\ 0, & \text{otherwise.} \end{cases} \tag{24}$$

The occupancy count for ensemble member j and for time period P_k, denoted as $O_j(P_k)$, is obtained as the sum of the occupancies of the different flights

$$O_j(P_k) = \sum_{i=1}^{m} O_{ij}(P_k). \tag{25}$$

Again, from these n values of occupancy count, the mean, maximum, and minimum values ($\bar{O}$, O_{max}, and O_{min}, respectively) can be obtained for the time period

$$\bar{O}(P_k) = \frac{1}{n}\sum_{j=1}^{n} O_j(P_k), \tag{26}$$

$$O_{max}(P_k) = \max_j O_j(P_k), \tag{27}$$

$$O_{min}(P_k) = \min_j O_j(P_k). \tag{28}$$

The dispersion of the occupancy count, $\Delta O(P_k)$, is defined as follows

$$\Delta O(P_k) = O_{max}(P_k) - O_{min}(P_k). \tag{29}$$

The probability of the occupancy count O being greater than a given value a for time period P_k is obtained from the number of occupancy counts $O_j(P_k)$ that are greater than this value, as follows

$$P[O(P_k) > a] = \frac{\text{number of } O_j(P_k) > a}{n}. \tag{30}$$

According to Eq. (24), the occupancy of the ATC sector by a flight during time period P_k depends not only on the entry time $t_{ij,E}$ but also on the exit time $t_{ij,X}$. The uncertainty in the exit time is the result of the uncertainty of the flight before entering the sector and the uncertainty of the flight while it is inside the sector. For one particular flight, the uncertainty in the exit time is expected to increase due to meteorological reasons when:

- the forecasting horizon increases,
- the aircraft flies over regions with high uncertainty before exiting the sector, and
- the aircraft travels a large distance before exiting the sector.

Therefore, taking into account the previous factors and those that affect the entry time (see Section 3.3), the uncertainty in the occupancy count is expected to increase when:

- the occupancy count is computed far in advance,
- the aircraft are affected by meteorological phenomena with large uncertainty before entering the sector and/or inside the sector,
- the traffic is composed of many flights arriving from distant locations, and
- the traffic is composed of many flights that cover a large distance inside the sector.

4 Application Example

In this section, an application example is provided to show the potentiality of the methodology presented in Section 3. In this application, the demand of an ATC sector is analysed for a whole day (from 00:00 to 24:00) when predicted the day before (at 00:00). Firstly, in Section 4.1, the traffic scenario is described, in terms of ATC sector, flights, and weather forecasts to be considered. In Section 4.2, the trajectory predictor developed for this application is described. Finally, in Section 4.3, the results are presented and analysed.

4.1 Traffic scenario

ATC sector

The ATC sector LECMSAU, located in the Northwest of Spain, see Figure 3, is considered in this application. The airspace of this sector can be described as one prism; it ranges from FL345 to FL 460, and the coordinates of the vertices that define the lateral boundary have been obtained from Eurocontrol's Network Strategic Tool (NEST) for the Aeronautical Information Regulation and Control (AIRAC) cycle 1701. The declared capacity of this sector (i.e., the maximum number of flights entering the sector per hour) is 36 flights/hour, also obtained from NEST and AIRAC cycle 1701.

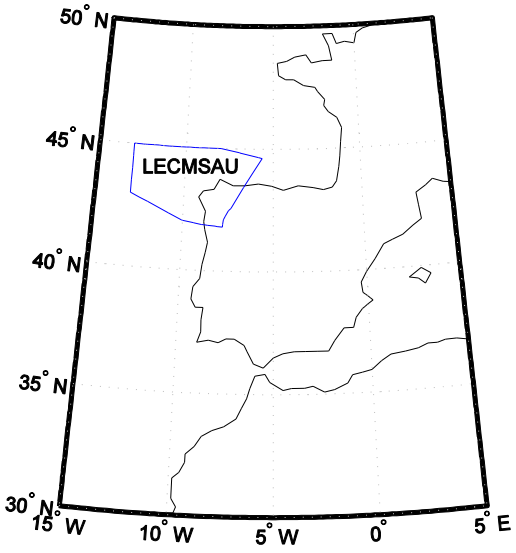

Figure 3. Geographical location of ATC sector LECMSAU.

Flights

In this application, the traffic that planned to cross this sector between 00:00 and 24:00 on 07 January 2017 is analysed. This traffic is retrieved from NEST software (AIRAC cycle 1701), and it corresponds to the last filed flight plan from the airlines (i.e., initial trajectories, according to NEST nomenclature). It is considered that each flight has a fixed route, provided by its flight plan, the same for all EPS members. As agreed by the consortium members in the Steering Board 1, only cruise trajectories at constant pressure altitude are assumed in TBO-Met.

A total number of 468 flights is obtained for this date and ATC sector. However, four of these flights are discarded, those flights arriving or departing to/from LEST airport (Santiago de Compostela). The reason is that, under the hypothesis of flying at constant pressure altitude, if they depart from LEST they instantly appear inside the sector and if they arrive to LEST they instantly disappear, not crossing the sector boundaries. Therefore, the entry or exit times are not defined for these aircraft if constant pressure altitude is assumed. Thus, a total number of 464 flights is considered in this application.

The routes followed by the 464 flights, defined by the coordinates of their waypoints, are shown in Figure 4. They are represented from the departure airports to the exit points of the sector (since the routes from the exit points to the arrival airports are not of interest in this analysis, they are not represented). This traffic is composed of short flights (departing from Portugal, Spain, and France), medium flights (mainly flights from the Canary Islands, the British Isles, and the Scandinavian Peninsula), and long flights (from America).

The relative frequency of the distance between the departure airport and the entry point is shown in Figure 5. Approximately, 9% of the flights travel less than 500 km before entering the sector, 26% between 500 and 1000 km, 21% between 1000 and 1500 km, 31% between 1500 and 2000 km, and 13% more than 2000 km. This represents an equilibrated mix of flights with different distances.

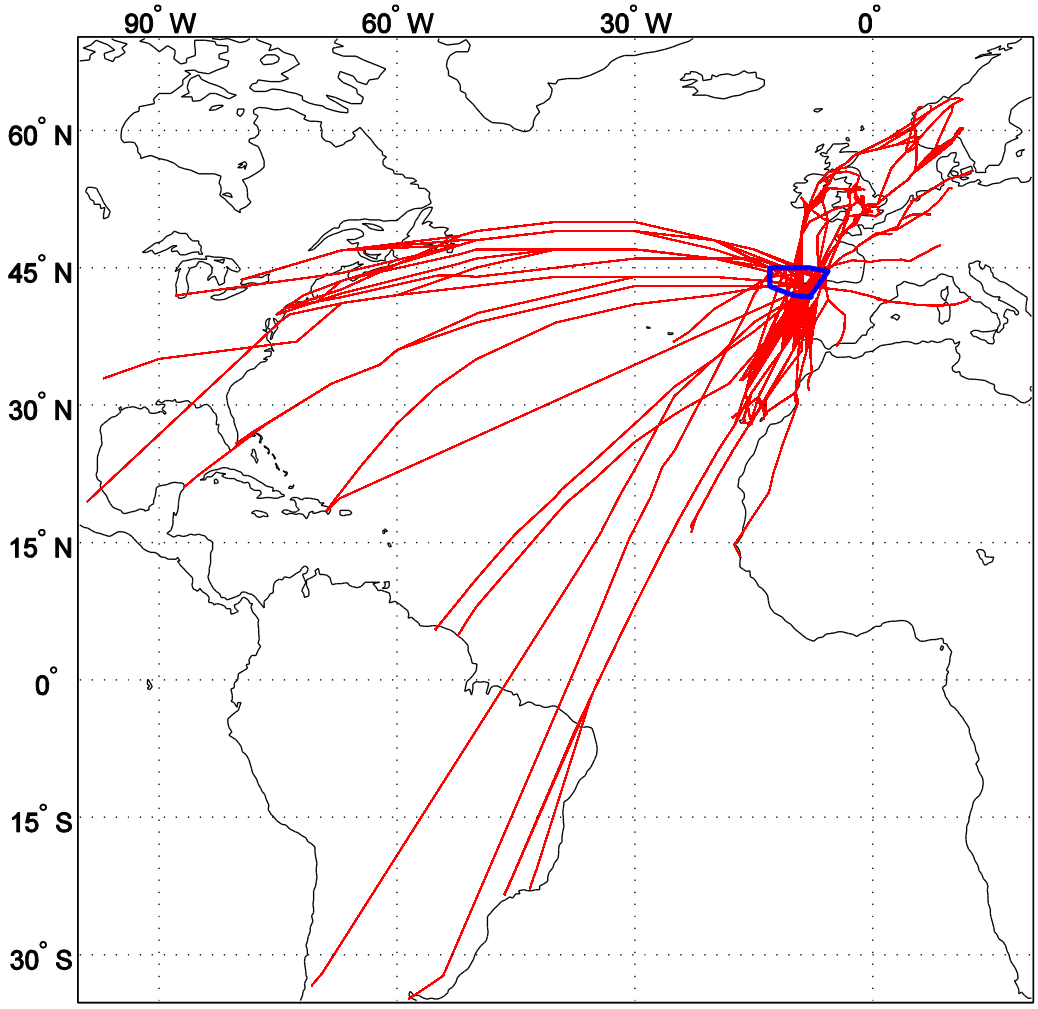

Figure 4. Traffic crossing LECMSAU on 07 January 2017 according to flight plans.

The trajectory predictor described in Section 4.2 requires the following information for each flight:

- departure time: which is obtained from NEST;
- coordinates of the waypoints that define the route: which are obtained from NEST;
- altitude: since in TBO-Met only cruise trajectories are considered, the pressure altitude has been fixed to 36000 ft for all aircraft and the whole flight (from origin to destination);
- airspeed: the average cruise Mach provided by Eurocontrol's Base of Aircraft Data (BADA) 3.13 for the aircraft model that performs the flight is considered for the whole flight (from origin to destination), ranging from 0.70 to 0.85.

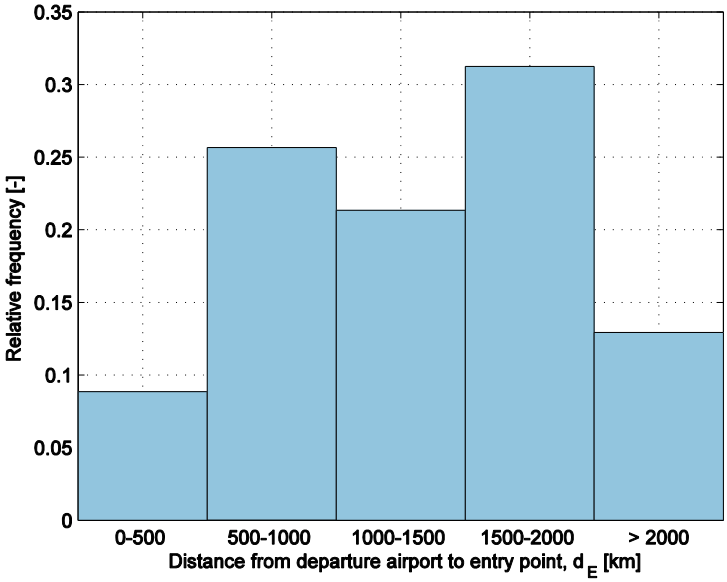

Figure 5. Relative frequency of the distance between the departure airport and the entry point.

Weather forecasts

In this application, the meteorological uncertainty is retrieved from the European Centre for Medium-Range Weather Forecasts. In particular, the weather forecast ECMWF-EPS, composed of 51 members, is used. It is considered that the analysis is performed the day before the operation; thus, the forecasts released at 00:00 on 06 January 2017 are considered. The meteorological uncertainty

According to the initial trajectories retrieved from NEST, the earliest flight departs at 17:25 on 06 January and, as a reference, the latest flight arrives to its destination at 04:00 on 08 January. Taking into account these times, the forecasts with time steps of 12, 18, 24, 30, 36, 42, 48, and 54 hours are considered in this application.

In agreement with the coordinates of the route waypoints, the forecasts are retrieved for a coverage area which ranges from 35 degrees South to 70 degrees North, and from 100 degrees West to 55 degrees East. The spatial grid resolution is 0.25 degrees.

According to the cruise altitude chosen for all flights (36000 ft), the forecasts are retrieved for the pressure level 200 hPa.

The meteorological variables required by the trajectory predictor described in Section 4.2 are the zonal and the meridional winds (winds along the West-East and South-North directions, respectively), and the air temperature.

In Figures 6 to 11, the average and dispersion of the meridional wind, the zonal wind, and the air temperature are shown for the forecast corresponding to the time instant 12:00 on 07 January. The

dispersion is measured as the difference between the maximum and the minimum values at each geographic location. Notice that, since the entry and occupancy counts are affected by the uncertainty the flights encounter before entering and inside the sector (see Sections 3.3 and 3.4), the area represented in Figures 6 to 11 is the same area represented in Figure 4, which covers the trajectories of the flights that enter LECMSAU.

The average meridional wind, see Figure 6, ranges approximately between -30 m/s (South direction) and 40 m/s (North direction). High values of the wind are found at the East coast of North America, and a high variation (approximately 70 m/s) is found between the Canary Islands and the Azores. The average zonal wind, see Figure 7, is larger than the meridional wind, ranging approximately between -20 m/s (West direction) and 70 m/s (East direction). The zonal wind is therefore the main contributor to the existence of jet streams. The larger values are found again at the East coast of North America, and at the Northwest of Africa.

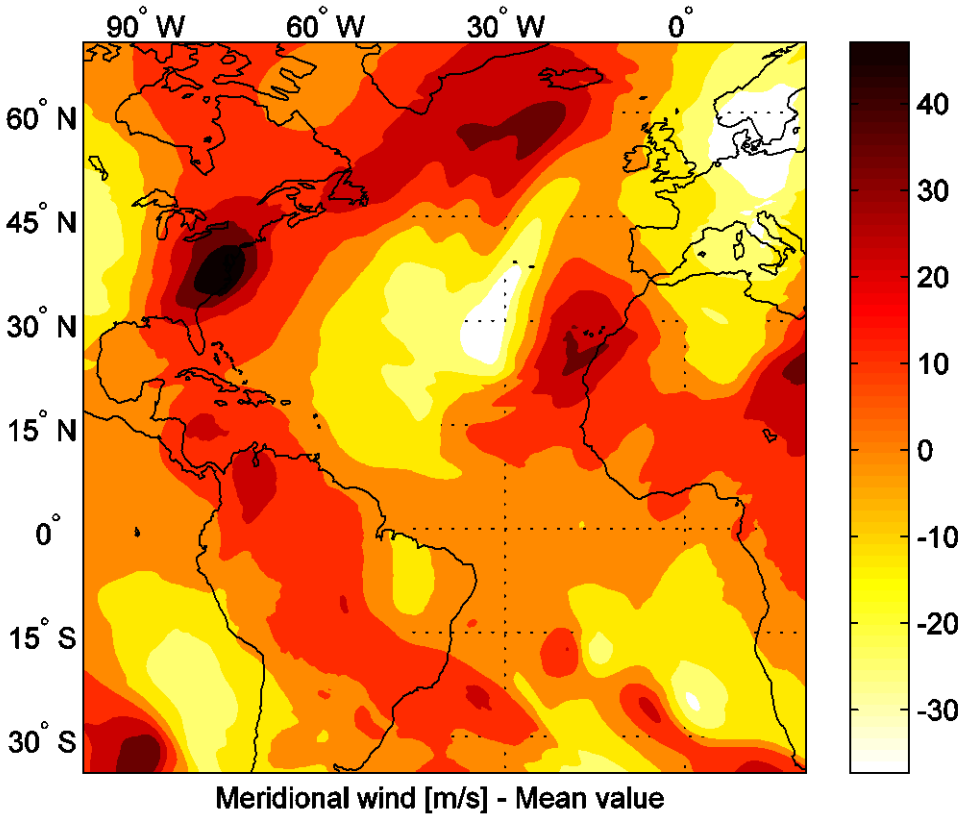

Figure 6. Average meridional wind, ECMWF-EPS released at 00:00, 06/01/17, step 36 hours.

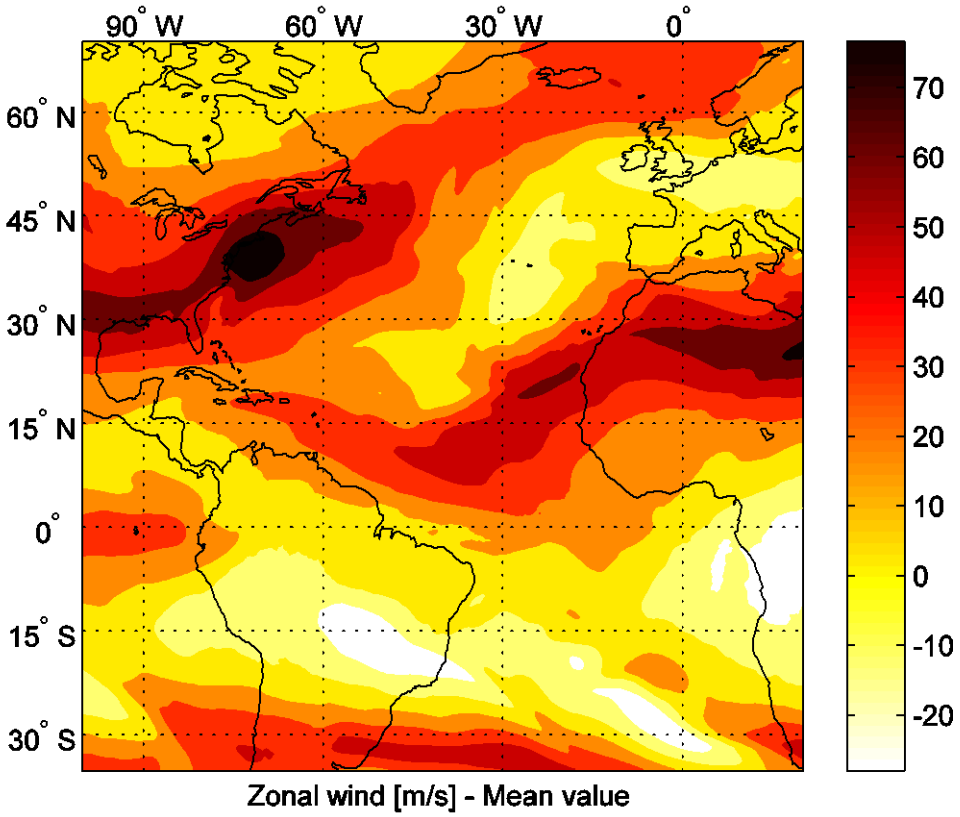

Figure 7. Average zonal wind, ECMWF-EPS released at 00:00, 06/01/17, step 36 hours.

The dispersion of the meridional and zonal winds is shown in Figures 8 and 9, respectively. In both cases, the dispersion can be rather large, with maximum values above 40 m/s. The geographic areas affected by high uncertainty are approximately the same in both cases. In particular, the following regions can be highlighted: 1) the East coast of North America and the North Atlantic, affecting flights from North America to Europe, and 2) South America and the Atlantic Ocean near the Equator, affecting flights from South America to Europe.

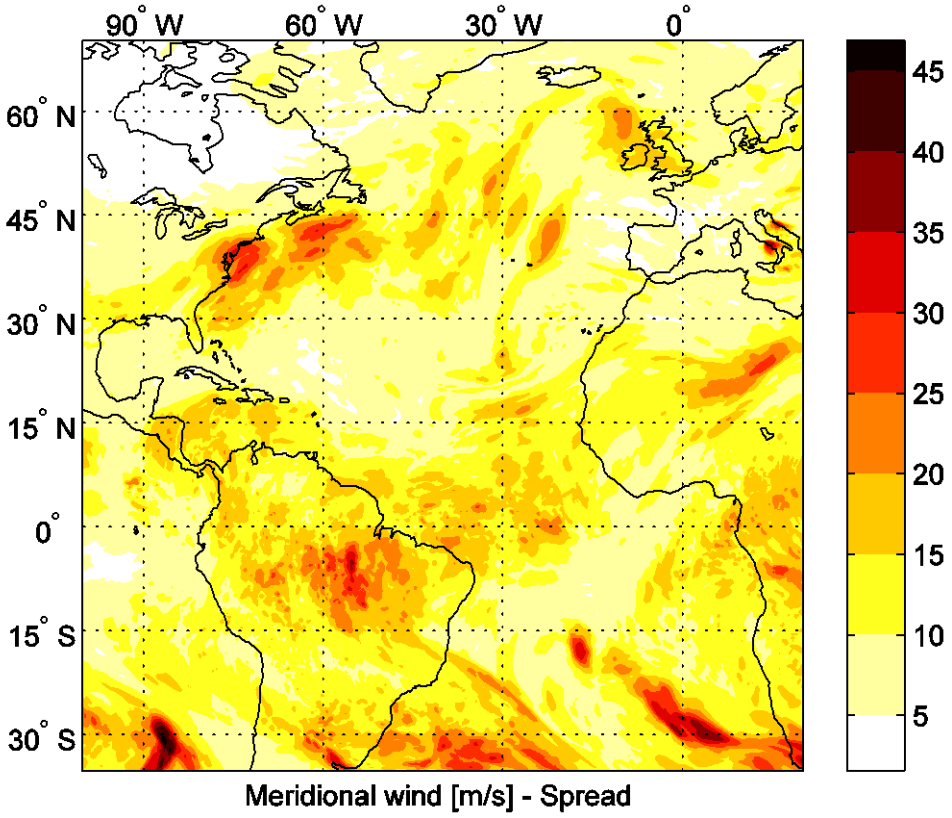

Figure 8. Dispersion of the meridional wind, ECMWF-EPS released at 00:00, 06/01/17, step 36 hours.

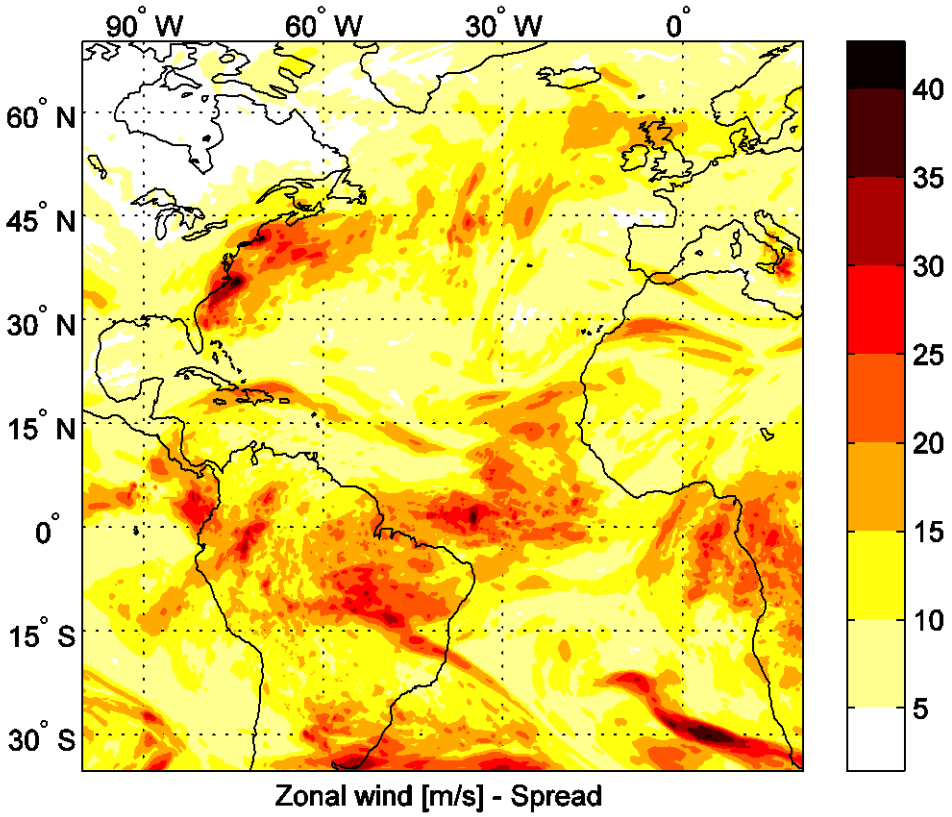

Figure 9. Dispersion of the zonal wind, ECMWF-EPS released at 00:00, 06/01/17, step 36 hours.

The average air temperature is presented in Figure 10. It can be seen that there is a cold area at the North Atlantic (approximately -65 ˚C), and a hot area very close to it, at the Labrador Peninsula and Greenland (approximately -45 ˚C). The dispersion at the North Atlantic is approximately 10 ˚C, see Figure 11.

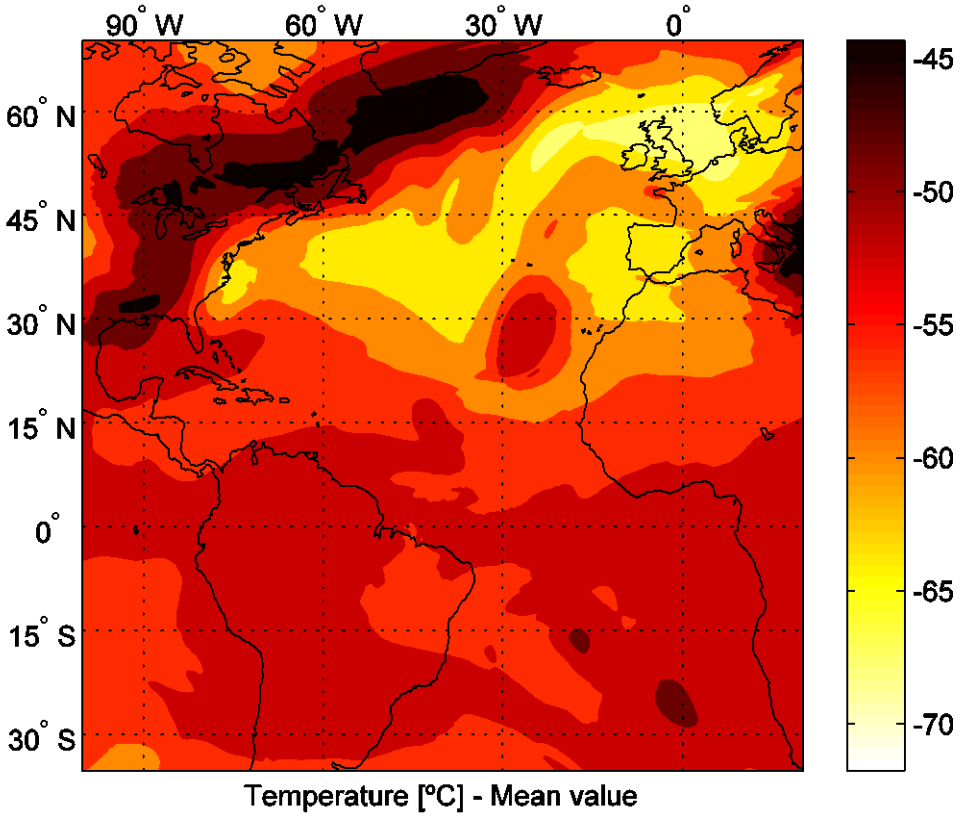

Figure 10. Average air temperature, ECMWF-EPS released at 00:00, 06/01/17, step 36 hours.

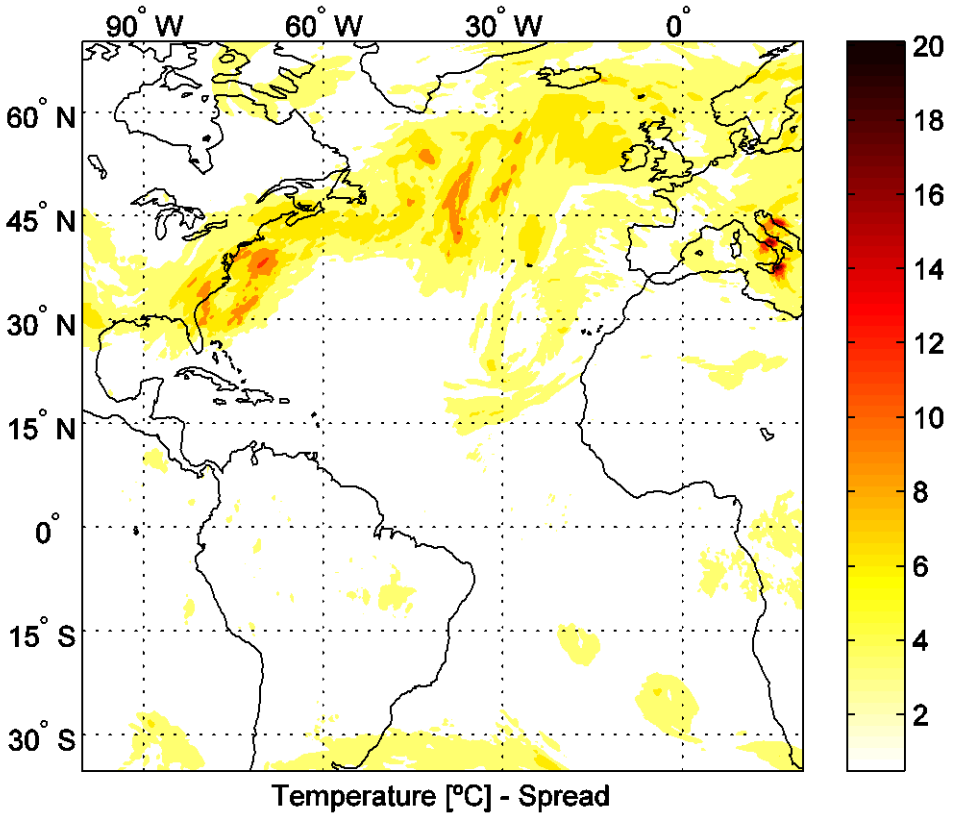

Figure 11. Dispersion of the air temperature, ECMWF-EPS released at 00:00, 06/01/17, step 36 hours.

4.2 Trajectory predictor

As indicated in Section 3, the trajectory predictor determines the aircraft trajectory for each flight and for each possible atmospheric scenario. As the coordinates of the waypoints defining the route of each flight are given, the objective of the trajectory predictor is to provide, for each flight and for each forecast member, a list of discrete times: the estimated times over the waypoints when variable horizontal winds and variable air temperature are encountered.

In this application a Spherical Earth is considered, with mean radius $R_E = 6371$ km.

Characterization of the routes

A trajectory is considered to be composed of several cruise segments connecting the given waypoints that define the route. Each one of these segments is defined by a constant course, and is flown at constant Mach number and constant pressure altitude.

For flight i ($i = 1, \dots, m$) and for segment k ($k = 1, \dots, p_i$, where p_i is the number of segments of the route), the longitude and latitude of the waypoints that define the segment are denoted as $\lambda_i^{[k-1]}$, $\lambda_i^{[k]}$, $\phi_i^{[k-1]}$ and $\phi_i^{[k]}$, respectively. For segment k, the course $\psi_i^{[k]}$ and the segment length $l_i^{[k]}$ can be computed from the following navigation equations:

$$\tan\psi_i^{[k]} = \frac{\lambda_i^{[k]} - \lambda_i^{[k-1]}}{\ln\left[\dfrac{\tan\left(\pi/4 - \phi_i^{[k-1]}/2\right)}{\tan\left(\pi/4 - \phi_i^{[k]}/2\right)}\right]} \tag{31}$$

$$l_i^{[k]} = \begin{cases} \dfrac{R_E\left(\phi_i^{[k]} - \phi_i^{[k-1]}\right)}{\cos\psi_i^{[k]}}, & \text{if } \phi_i^{[k]} \neq \phi_i^{[k-1]}, \\ R_E\cos\phi_i^{[k-1]}\left|\lambda_i^{[k]} - \lambda_i^{[k-1]}\right|, & \text{if } \phi_i^{[k]} = \phi_i^{[k-1]}, \end{cases} \tag{32}$$

where it has been assumed that the 180th meridian is never crossed. Note that, if $\phi_i^{[k]} = \phi_i^{[k-1]}$, Eq. (31) becomes $\psi_i^{[k]} = \mathrm{sgn}\left(\lambda_i^{[k]} - \lambda_i^{[k-1]}\right)\frac{\pi}{2}$.

Taking the accumulated distance travelled over the Earth along the trajectory, r, as the independent variable, one can obtain the position of flight i at distance r, that is, the vector $\mathbf{x}_i(r) = [\lambda_i(r), \phi_i(r), h_i]$, from the equations of navigation along constant rhumb lines:

$$\phi_i(r) = \phi_i^{[k-1]} + \frac{r - r_i^{[k-1]}}{R_E}\cos\psi_i^{[k]}, \quad \text{if } r \in \left[r_i^{[k-1]}, r_i^{[k]}\right], \tag{33}$$

$$\lambda_i(r) = \begin{cases} \lambda_i^{[k-1]} + \tan\psi_i^{[k]}\ln\left[\dfrac{\tan\left(\dfrac{\pi}{4} - \dfrac{\phi_i^{[k-1]}}{2}\right)}{\tan\left(\dfrac{\pi}{4} - \dfrac{\phi_i(r)}{2}\right)}\right], & \text{if } \phi_i(r) \neq \phi_i^{[k-1]} \text{ and } r \in \left[r_i^{[k-1]}, r_i^{[k]}\right], \\ \lambda_i^{[k-1]} + \dfrac{l_i^{[k]}\,\mathrm{sgn}\left(\lambda_i^{[k]} - \lambda_i^{[k-1]}\right)}{R_E\cos\phi_i^{[k-1]}}, & \text{if } \phi_i(r) = \phi_i^{[k-1]} \text{ and } r \in \left[r_i^{[k-1]}, r_i^{[k]}\right], \end{cases} \tag{34}$$

where $r_i^{[k]}$ is the accumulated distance corresponding to the kth waypoint, given by $r_i^{[k]} = \sum_{q=1}^{k} l_i^{[q]}$ (for $k = 1, \dots, p_i$) and $r_i^{[0]} = 0$.

Atmospheric variables along the routes

The flights are supposed to be subject to variable meridional and zonal winds (horizontal winds), and variable air temperature. For member j ($j = 1, \dots, n$), these atmospheric variables are considered to be location and time dependent, and are denoted by $w_{m,j}(\lambda, \phi, h, t)$, $w_{z,j}(\lambda, \phi, h, t)$ and $T_j(\lambda, \phi, h, t)$,

respectively. Linear interpolation is performed to obtain meridional and zonal winds and air temperature for a specific location and time (i.e. for a given query point) from gridded values provided by the retrieved weather forecast.

Taking into account Eqs. (33-34), for flight i and for member j, one has:

$$w_{m,ij}(r,t) = w_{m,j}[\lambda_i(r), \phi_i(r), h_i, t], \tag{35}$$

$$w_{z,ij}(r,t) = w_{z,j}[\lambda_i(r), \phi_i(r), h_i, t], \tag{36}$$

$$T_{ij}(r,t) = T_j[\lambda_i(r), \phi_i(r), h_i, t]. \tag{37}$$

Furthermore, meridional and zonal winds can be transformed into along-track winds and crosswinds by a rotation of axes:

$$\begin{bmatrix} w_{ij}(r,t) \\ w_{c,ij}(r,t) \end{bmatrix} = \begin{bmatrix} \cos\psi_i^{[k]} & \sin\psi_i^{[k]} \\ -\sin\psi_i^{[k]} & \cos\psi_i^{[k]} \end{bmatrix} \begin{bmatrix} w_{m,ij}(r,t) \\ w_{z,ij}(r,t) \end{bmatrix}, \qquad \text{for } r \in \left[r_i^{[k-1]}, r_i^{[k]}\right]. \tag{38}$$

Note that the along-track wind is positive for tailwinds and the crosswind is positive if it blows from the left wing.

Kinematic equation of motion

The effects of the crosswinds are considered in a simplified manner, taking them into account in the kinematic equations, ignoring the lateral dynamics, and translating the crosswind into an equivalent headwind. This leads to a reduced ground speed for flight i and for member j, which is given by

$$V_{g,ij}(r,t) = \sqrt{\gamma R_g T_{ij}(r,t) M_i^2 - w_{c,ij}^2(r,t)} + w_{ij}(r,t). \tag{39}$$

where M_i is the constant Mach number for flight i, γ is the ratio of specific heats of the air and R_g is the gas constant of the air.

Finally, for flight i and for member j, the estimated times over the waypoints, namely $t_{ij}^{[k]}$ $(k = 0, \dots, p_i)$, can be determined by first solving the following initial value problem,

$$\begin{cases} \dfrac{dt_{ij}}{dr} = \dfrac{\left(1 + \dfrac{h_i}{R_E}\right)}{V_{g,ij}(r, t_{ij})} \\ t_{ij}(0) = t_i^{[0]} \end{cases} \tag{40}$$

where $t_i^{[0]}$ is the given departure time, and then evaluating at the accumulated distances corresponding to the waypoints: $t_{ij}^{[k]} = t_{ij}\left(r_i^{[k]}\right)$, for $k = 1, \dots, p_i$. Note that $t_{ij}^{[0]} = t_i^{[0]}$ for any forecast member.

4.3 Results

This section is organised as follows. First, the entry, exit, and occupancy times are analysed. Next, the entry and occupancy counts are presented for two different values of the step t_s and of the duration of the time period δt. Finally, the probability of exceeding the declared capacity of the sector is also presented for two different values of t_s and of δt.

Entry, exit, and occupancy times

The dispersion of the entry time, $\Delta t_{i,E}$, as a function of the distance to the entry point, $d_{i,E}$, for each flight is presented in Figure 12 (notice that, since in this application the route of each flight is the same for all the atmospheric realizations, then the distances $d_{ij,E}$, $d_{ij,X}$, and $d_{ij,O}$, are the same for all the ensemble members). As expected, the dispersion increases as the distance increases because the uncertainty is accumulated along the trajectories; flights arriving from distant locations present more uncertainty. The maximum value of the dispersion is 584 seconds, whereas the minimum value is 6 seconds.

It can be seen that there are flights with similar distances but different values of dispersion. For example, for $d_{i,E}$ approximately equal to 2000 km, the dispersion ranges between 119 and 206 seconds. As possible causes of these different values, the following ones can be highlighted:

- different routes (flights over regions of the airspace with different uncertainty),
- different effects of the same wind uncertainty on different flights (uncertainties in tail/headwinds have a higher impact than uncertainties in crosswinds),
- different departure times (the predictions for flights departing later are made with weather forecasts with larger time horizons, thus having a larger uncertainty), or
- different speeds (flights with lower values of Mach number and with headwinds are more sensitive to uncertainties in the wind, and flights with higher values of Mach number are more sensitive to uncertainties in the air temperature).

The relative frequency of the dispersion of the entry time is shown in Figure 13. In this application, 13% of the flights have a dispersion below 1 minute, 29% between 1 and 2 minutes, 39% between 2 and 3 minutes, 14% between 3 and 4 minutes, and 5% above 4 minutes.

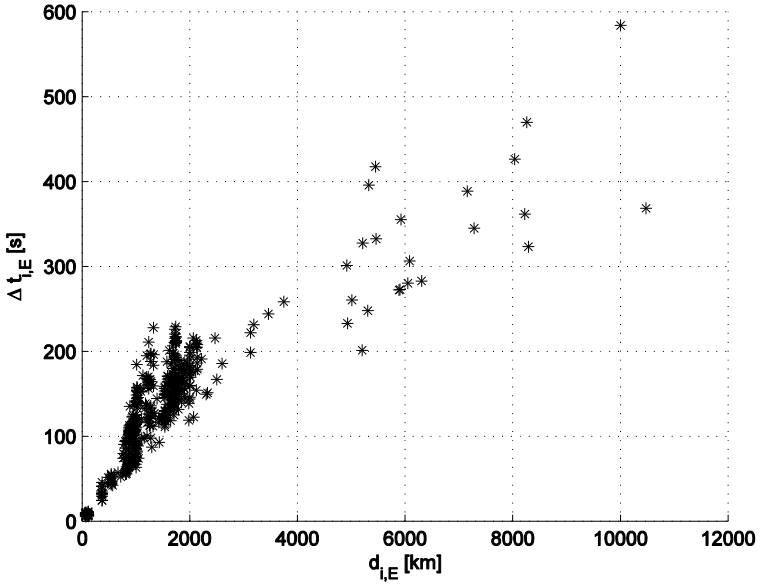

Figure 12. Dispersion of the entry time vs distance to the entry point.

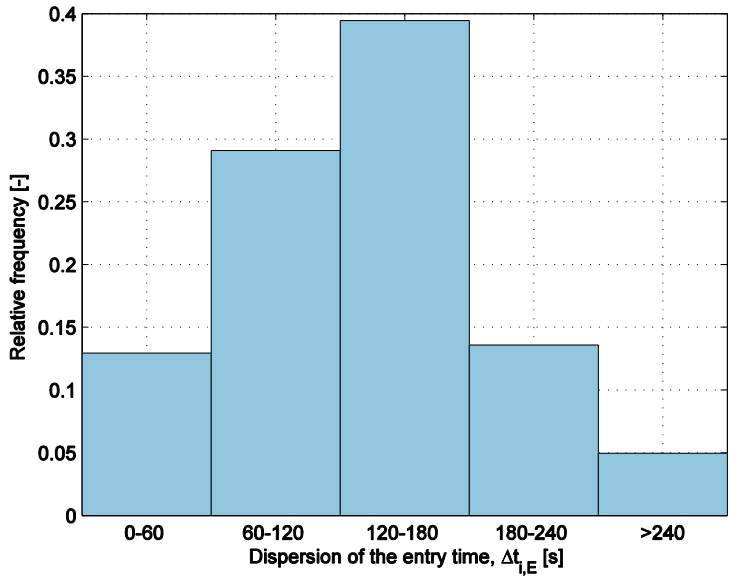

Figure 13. Relative frequency of the dispersion of the entry time.

The dispersion of the exit time, $\Delta t_{i,X}$, as a function of the distance to the exit point, $d_{i,X}$, is presented in Figure 14. This dispersion is slightly higher than the dispersion of the entry time; now 8% of the flights have a dispersion below 1 minute, 30% between 1 and 2 minutes, 39% between 2 and 3 minutes, 18% between 3 and 4 minutes, and 5% above 4 minutes, see Figure 15. This difference is due to the

uncertainty accumulated when flying inside the sector. Now, the maximum value of the dispersion is 586 seconds, whereas the minimum value is 36 seconds.

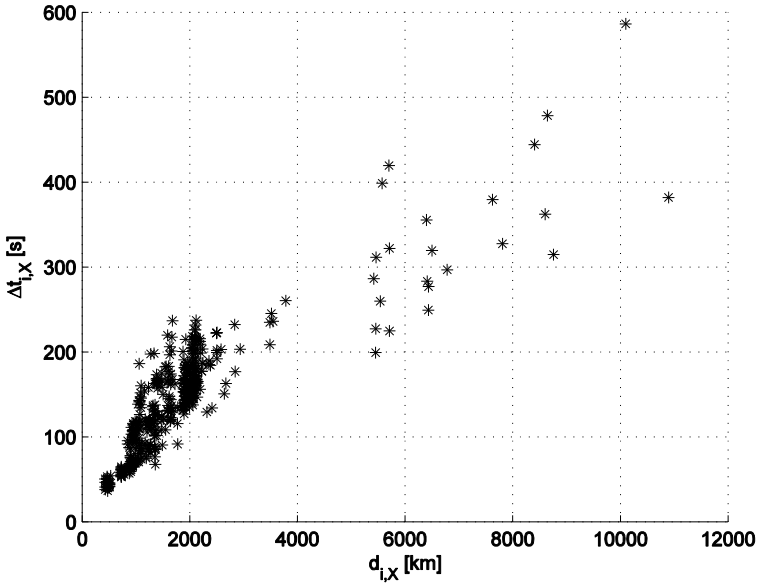

Figure 14. Dispersion of the exit time vs distance to the exit point.

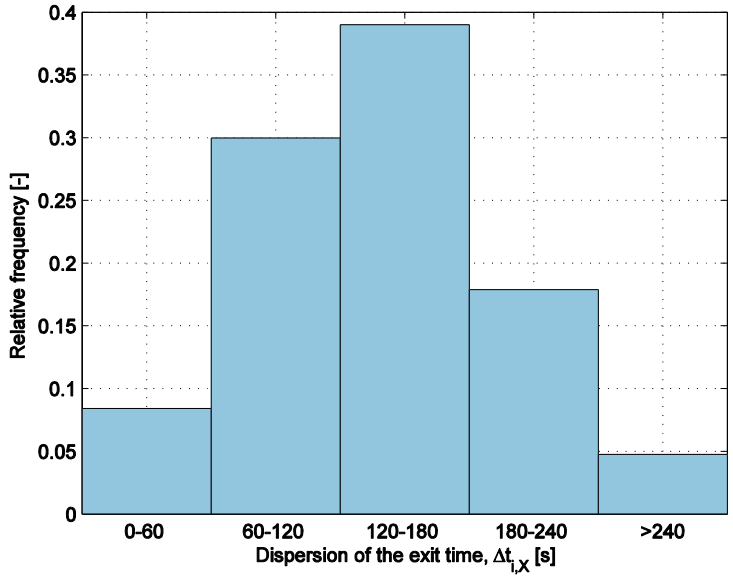

Figure 15. Relative frequency of the dispersion of the exit time.

The dispersion of the occupancy time as a function of the distance flown inside the sector is presented in Figure 16. Again, as expected, the dispersion increases as this distance increases. Approximately, 30% of the flights travel a distance smaller than 100 km, thus they accumulate a very small amount of

uncertainty inside the sector. The highest value of the dispersion is 54 seconds. The relative frequency of the dispersion of the occupancy time is shown in Figure 17: 30% of the flights have a dispersion below 10 seconds, 3% between 10 and 20 seconds, 25% between 20 and 30 seconds, 35% between 30 and 40 seconds, 6% between 40 and 50 seconds, and 1% above 50 seconds.

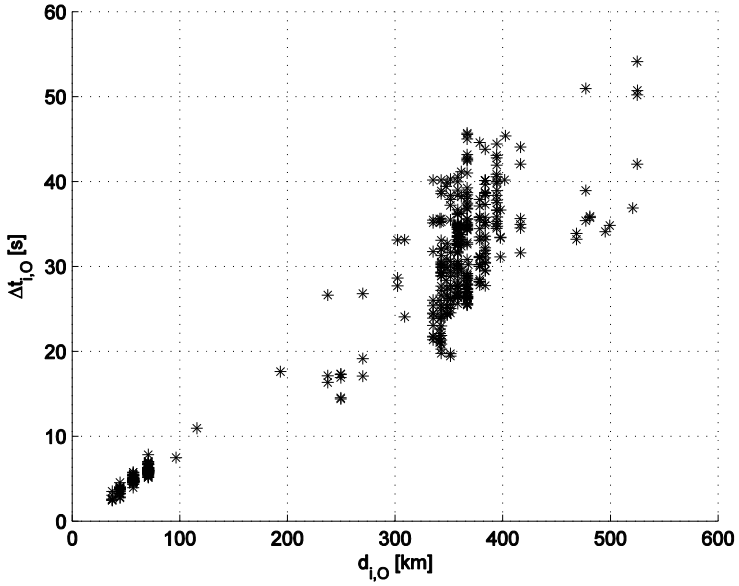

Figure 16. Dispersion of the occupancy time vs distance flown inside the sector.

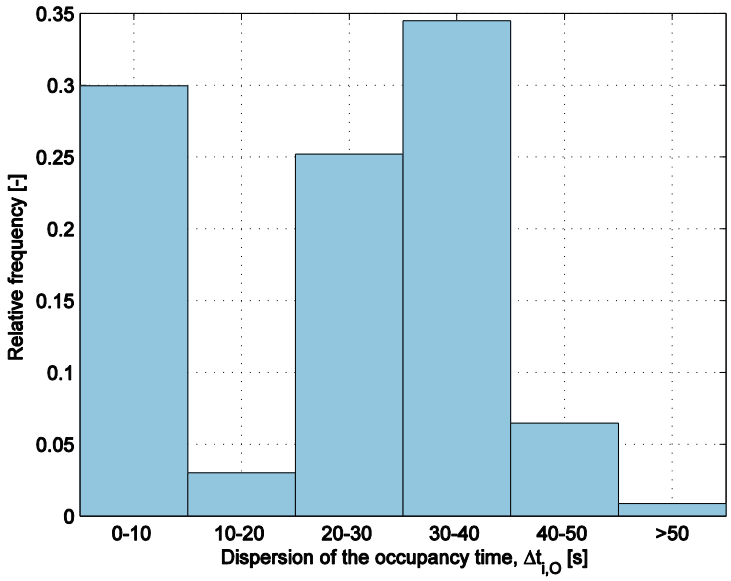

Figure 17. Relative frequency of the dispersion of the occupancy time.

Entry and occupancy counts

The maximum, average, and minimum values of the entry and occupancy counts for t_s =60 min and δt =60 min are shown in Figures 18 and 19, respectively (for each time interval, these figures display three superposed vertical bars: the minimum, mean, and maximum values of the entry count). The largest value of the mean entry count is 44.0 flights (for the time period 14:00-15:00), and the largest value of the mean occupancy count is 63.0 flights (for the same time period).

The uncertainty on these counts is on the spread of the number of flights. The difference between the maximum and the minimum values of the entry count is as large as 3 flights (for 15:00-16:00, 21:00-22:00, and 22:00-23:00), and for the occupancy count is also 3 flights (for 14:00-15:00, and 19:00-20:00). The dispersion of the entry count is shown in Figure 20. From this figure it can be observed that the dispersion is 3 flights for a total of 3 hours (in disjoint periods), 2 flights for 6 hours, 1 flight for 6 hours, and 0 flights for the remaining 9 hours. For the occupancy count, the dispersion is 3 flights for 2 hours, 2 flights for 7 hours, 1 flight for 6 hours, and 0 flights for the remaining 9 hours, as shown in Figure 21.

It is worth noting that, in this application, where only wind and air temperature uncertainties are considered, these uncertainties are rather large when compared, for example with the declared capacity; 3 flights compared with 36 flights/hour is about 8%. It is expected to obtain even larger values of uncertainty in these counts for scenarios that consider uncertainties on convective phenomena. These scenarios will be analysed in deliverable D5.2.

Taking into account that the declared capacity is 36 flights/hour (represented as a red line along with the entry count in Figure 18), this capacity is exceeded for time periods 08:00-09:00, 14:00-15:00, 16:00-17:00. In fact, according to NEST, an ATFCM regulation was activated (named SAU07) in the period 14:00-16:11 due to ATC capacity.

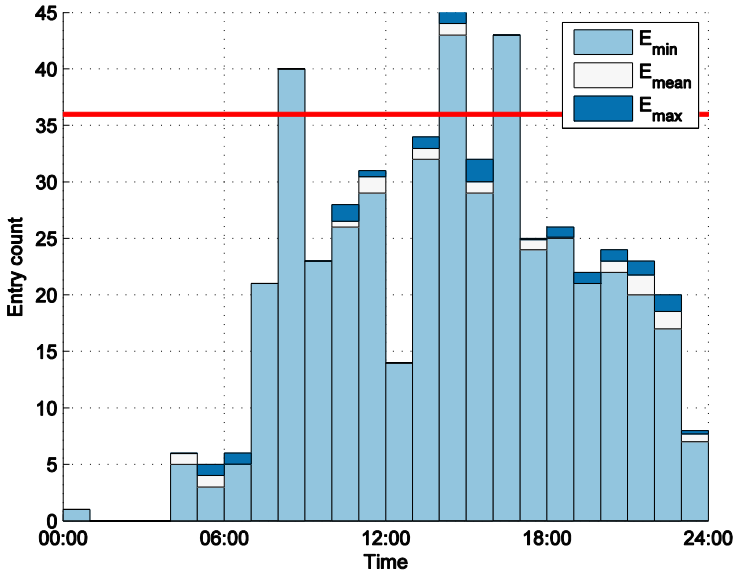

Figure 18. Entry count for $t_s = 60$ min and δt =60 min.

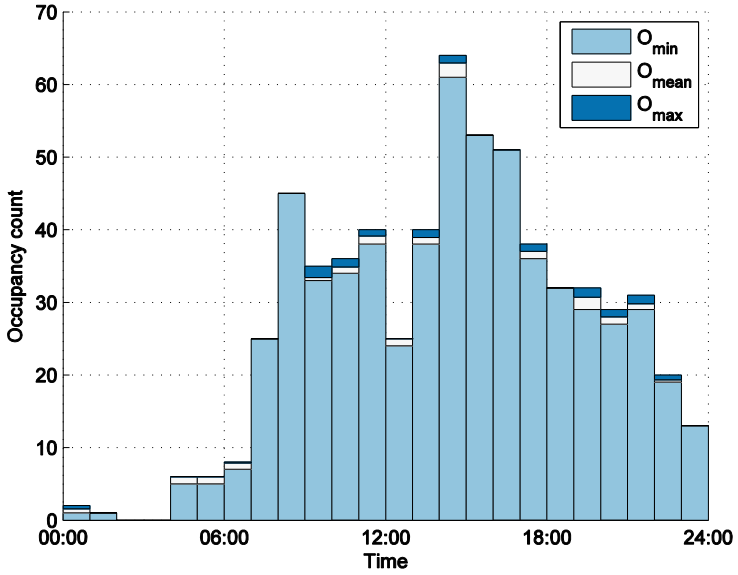

Figure 19. Occupancy count for $t_s = 60$ min and δt =60 min.

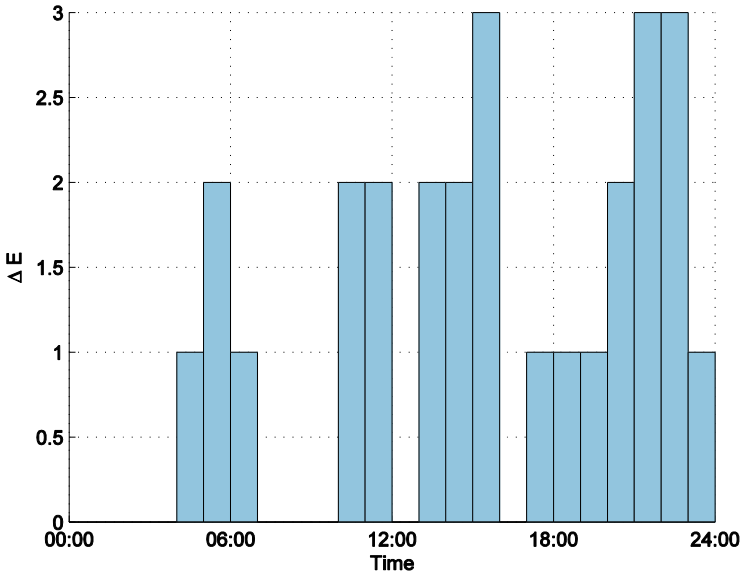

Figure 20. Dispersion of the entry count for $t_s = 60$ min and δt =60 min.

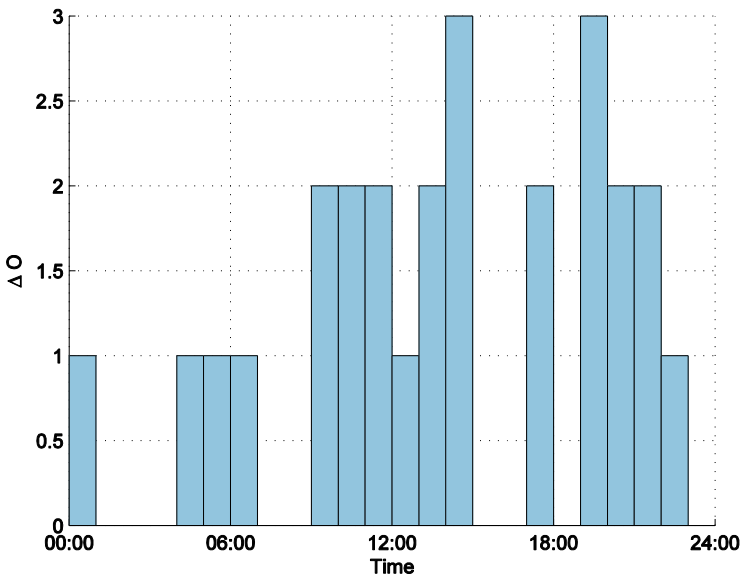

Figure 21. Dispersion of the occupancy count for $t_s = 60$ min and δt =60 min.

Now, in Figures 22 and 23, the entry and occupancy counts are shown for shorter time periods, t_s =10 min and δt =10 min. Assuming that the capacity is 6 aircraft/10 minutes (one sixth of the declared capacity, 36 aircraft/hour), it is seen that this capacity is clearly exceeded multiple times.

When shortening the duration of the time period, the average values of the counts are proportionally reduced, but it can be seen that the dispersions are not, they remain with values around 2-3 aircraft; thus, the uncertainty is relatively more important. Now, the largest dispersion on the entry count is 4 flights (for 22:30-22:40 and 22:40-22:50), and for the occupancy count is also 4 flights (for 14:40-14:50, 20:40-20:50, and 22:30-22:40). The dispersion of the entry count is shown in Figure 24; it can be obtained that the dispersion is 4 flights for a total of 0.33 hours, 3 flights for 1.83 hours, 2 flights for 5.83 hours, 1 flight for 8 hours, and 0 flights for the remaining 8 hours. The dispersion of the occupancy count, see Figure 25, is 4 flights for 0.50 hours, 3 flights for 1.83 hours, 2 flights for 6.17 hours, 1 flight for 7.5 hours, and 0 flights for the remaining 8 hours.

If the duration of the time period is reduced to 1 minute, then the maximum dispersion is 5 flights for the entry count and 6 flights for the occupancy count. Thus, it can be seen that, as expected, the maximum value of dispersion increases as the duration of the time period decreases.

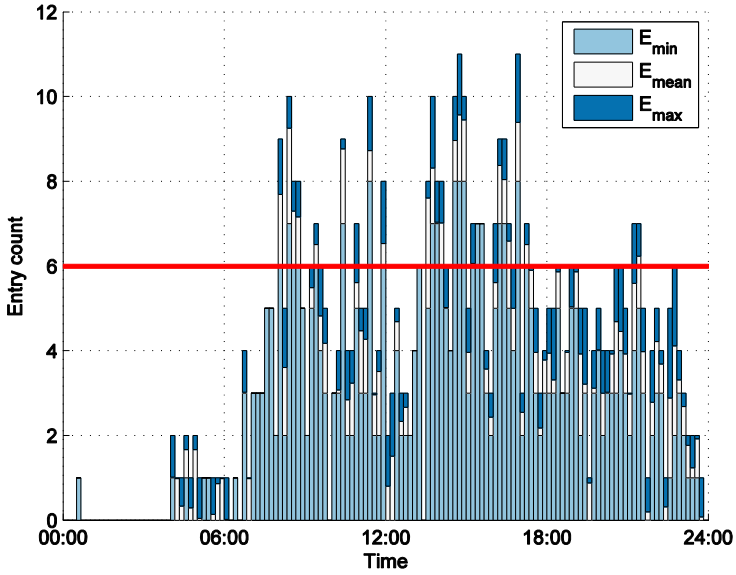

Figure 22. Entry count for t_s =10 min and δt =10 min.

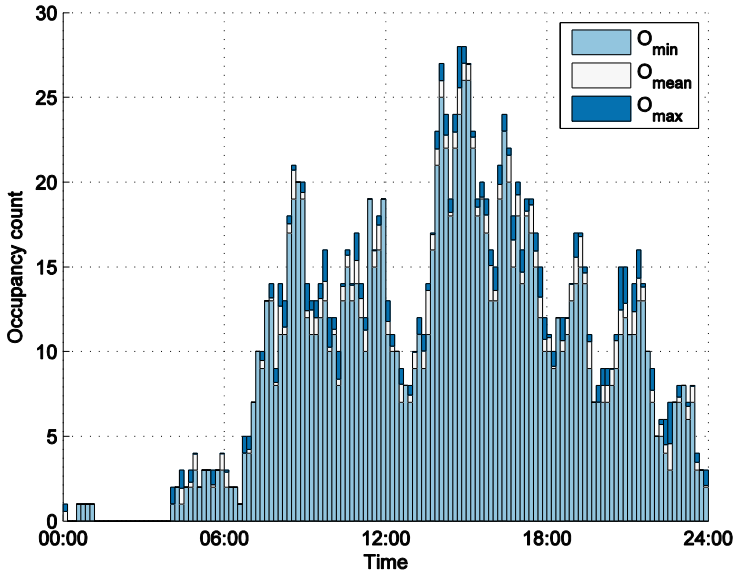

Figure 23. Occupancy count for t_s =10 min and δt =10 min.

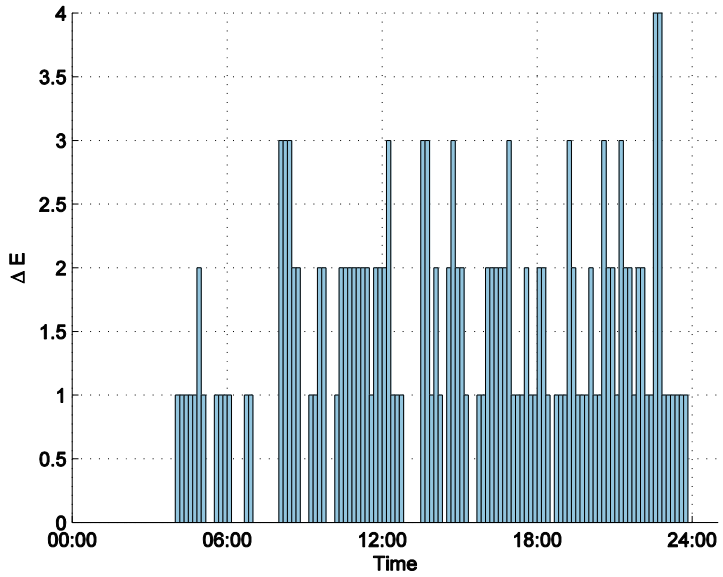

Figure 24. Dispersion of the entry count for t_s =10 min and δt = 10 min.

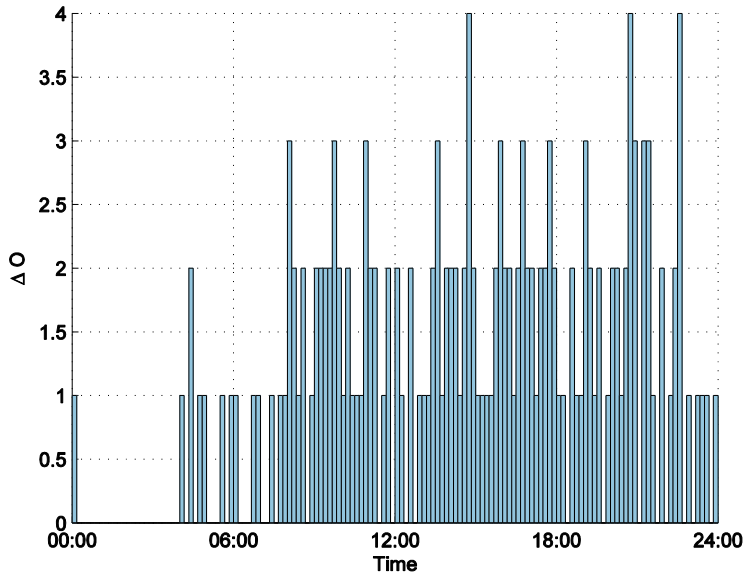

Figure 25. Dispersion of the occupancy count for t_s =10 min and δt = 10 min.

Probability of exceeding the declared capacity

The probability of the entry count being greater than the declared capacity (36 aircraft/hour) for t_s =60 min and δt =60 min is shown in Figure 24. This probability takes the value 1 for time periods 08:00-09:00, 14:00-15:00, and 16:00-17:00, and 0 otherwise. Therefore, there is a total assurance in having a capacity shortfall for these periods. Since the severity of the ATFCM measures depends on

the value of the capacity shortfall, this deficit should be quantified. In this application, this maximum deficit is considered, measured as the difference between the maximum entry count and the declared capacity. It is marked by asterisks in Figure 24 (this maximum deficit can be easily identified in Figure 18 by the periods with higher maximum entry counts). It can be seen that the period 14:00-15:00 is the most severe, its maximum deficit is 9 flights.

The probability of exceeding a capacity of 6 aircraft/10 minutes for $t_s = 10$ min and δt =10 min is shown in Figure 25. In this case, intermediate values of probability are found. For example, if a probability threshold of 0.8 is considered, this value is exceeded in 18 different time periods, a total of 3 hours. In Figure 25, the capacity deficit is only shown for periods with a probability value above 0.8; the periods 14:40:14:50 and 16:50-17:00 are the most severe, with a maximum deficit of 5 flights.

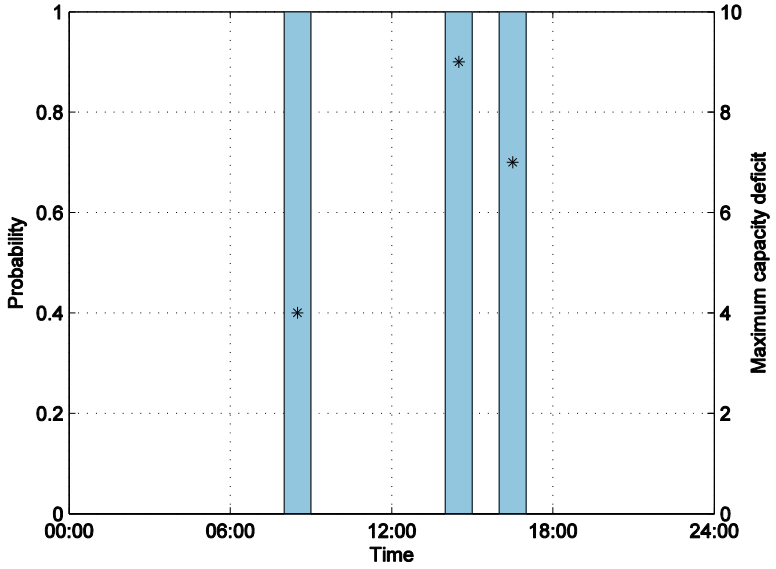

Figure 26. Probability of exceeding a capacity of 36 flights/hour (continuous line) and maximum capacity deficit (asterisks), for t_s =60 min and δt =60 min.

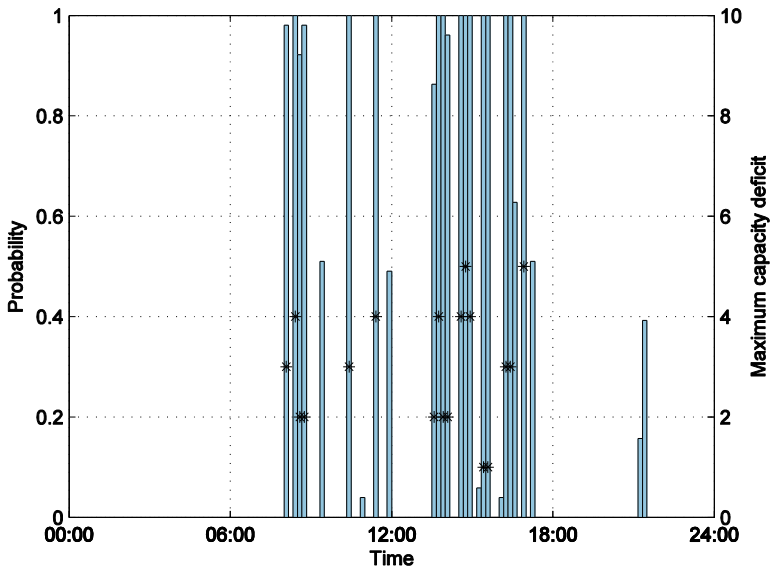

Figure 27. Probability of exceeding a capacity of 6 flights/hour (continuous line) and maximum capacity deficit (asterisks), for t_s =10 min and δt =10 min.

5 Conclusions

A methodology to assess the uncertainty of sector demand when meteorological uncertainty is taken into account has been presented in this deliverable. This methodology requires to define a scenario in terms of Air Traffic Control sector, flights, and weather forecasts. In TBO-Met, the meteorological uncertainty is provided by Ensemble Prediction systems (EPS) for mid-term planning and by EPS and Nowcasts for short-term planning and execution. A trajectory predictor computes, for each flight and for each possible atmosphere realization, a different aircraft trajectory. The methodology is general, it can be applied to both sources of weather uncertainty and to any forecast horizon. The computed trajectories along with the information of the sector, are then used to analyse the sector demand.

The analysis is based on the statistical characterization of the entry and exit times of the flights to/from the sector, and of the entry and occupancy counts. Mean, maximum, and minimum values, and the spread of these times and counts, are obtained. The probability of the counts of exceeding given thresholds is also obtained, which can be used to represent the probability that the demand exceeds the declared capacity of the sector. This probability can be useful in the Demand-Capacity Balancing process. The higher the value of the probability and the capacity deficit, the more severe the Air Traffic Flow and Capacity Management measure to be considered.

The statistical characterization has been performed under certain general hypotheses. Two of them can be highlighted: the geometry of the sector is considered to be fixed over time, and the aircraft trajectories cross the sector only once. The opening and/or closing of sectors would result in transient effects, and the returning of aircraft to their departure airport is an uncommon practice. These two hypotheses do not impact the objective of Work Package 5: to help in the understanding of how weather uncertainty is propagated from the trajectory scale to the traffic scale. In future extensions of the project, oriented to a practical implementation, these two hypotheses could be relaxed and the statistical characterization appropriately extended.

A realistic application example has been provided in this deliverable: the demand of the ATC sector LECMSAU is analysed for a whole day when predicted the day before. The meteorological uncertainty is obtained from the ensemble forecast ECMWF-EPS. In this application, cruise flights at constant pressure altitude are assumed. A trajectory predictor that takes into account the uncertainty in wind and air temperature has been developed for this application.

In this particular example, it has been found that, because uncertainty is accumulated along the flight, the uncertainty in the entry, exit, and occupancy times increases as the distance travelled by the aircraft to the entry point, to the exit point, and inside the sector, respectively, increases. Also, it has been found that the uncertainty in the entry count is large, about 8%, when compared with the declared capacity of the sector. Even larger values of uncertainty are expected to be found when

uncertainty on convective phenomena will be considered, which will be tackled in later stages of the project.

This application has shown the potentiality of the methodology. In deliverable D5.2, it will be applied to quantify the effects of weather uncertainty on the sector demand at the pre-tactical and tactical phases, and to quantify the benefits of improving the predictability of individual trajectories on the predictability of sector demand.

6 References

[1] *Grant Agreement number: 699294 — TBO-MET — H2020-SESAR-2015-1.*

[2] "TBO-Met Deliverable 2.1, Requirements and Concept for EPS Processing," Edition 00.01.01, September 2016.

[3] "TBO-Met Deliverable 2.3, Requirements and Concept for Nowcast Processing," Edition 00.01.00, February 2017.

[4] World Meteorological Organization, "Guidelines on Ensemble Prediction Systems and Forecasting," WMO-No. 1091, 2012.

[5] M. Steiner, R. Bateman, D. Megenhardt, Y. Liu, M. Xu, M. Pocernich and J. A. Krozel, "Translation of ensemble weather forecasts into probabilistic air traffic capacity impact," *Air Traffic Control Quarterly,* vol. 18, no. 3, pp. 229-254, 2010.

[6] P. Li, W. Wong, K. Chan and E. Lai, "SWIRLS – An Evolving Nowcasting System," *Technical Note No. 100, Hong Kong Observatory,* pp. 1-33, 2000.

[7] K. Kober and A. Tafferner, "Tracking and nowcasting of convective cells using remote," *Meteorologische Zeitschrift,* vol. 1, no. 18, pp. 75-84, 2009.

[8] M. Dalichampt and C. Plusquellec, "Hourly Entry Count versus Occupancy Count – Definitions and indicators (I). EEC Note No. 15/07," Eurocontrol Experimental Centre, 2007.

[9] "TBO-Met Deliverable 1.1, Project Management Plan," Edition 00.01.02, November 2016.

[10] "TBO-Met Deliverable 4.1, Efficiency/predictability trade-off of 4D trajectories at pretactical level," Edition 00.01.00, February 2017.